Available online at www.sciencedirect.com
ScienceDirect
Journal of Molecular Catalysis A: Chemical 261 (2007) 53–63
JOURNAL OF MOLECULAR CATALYSIS A: CHEMICAL
www.elsevier.com/locate/molcata

Activation process of 3-alkyl-substituted *ansa*-bis(indenyl) zirconocenes by MAO

Carlos Alonso-Moreno [a], Antonio Antiñolo [a], Fernando Carrillo-Hermosilla [a], Pedro Carrión [a], Ana M. Rodríguez [a], Antonio Otero [a,*], José Sancho [b]

[a] *Departamento de Química Inorgánica, Orgánica y Bioquímica, Facultad de Ciencias Químicas, Universidad de Castilla-La Mancha, Campus Universitario de Ciudad Real, 13071-Ciudad Real, Spain*
[b] *Centro Tecnológico de Repsol-YPF, Carretera de Extremadura, km. 18, 28931-Móstoles, Spain*

Received 20 April 2006; received in revised form 13 July 2006; accepted 14 July 2006
Available online 1 September 2006

Abstract

The *ansa*-indene compound {1-Me_2Si(3-$C_9H_6Et)_2$} (**1**) was prepared by alkylation of the unsubstituted *ansa*-indene. This compound was converted, by reaction with *n*BuLi, to the dilithium compound [Li_2{1-Me_2Si(3-$C_9H_5Et)_2$}] (**2**). *ansa*-Zirconocene [Zr{1-Me_2Si(3-η^5-$C_9H_5Et)_2$}Cl_2] (**3**) was prepared by the reaction of $ZrCl_4$ with **2** in ether/toluene at −78 °C. The molecular structure of *meso*-**3** was determined by single crystal X-ray diffraction studies. The *ansa*-zirconocene **3** exhibits a greater activity in ethylene polymerization than reference complexes such as [Zr{1-Me_2Si(η^5-$C_9H_6)_2$}Cl_2] and [Zr{1-C_2H_4(η^5-$C_9H_5)_2$}Cl_2] and, in addition, it maintained a reasonable level of activity after 12 h of contact with MAO solution. Furthermore, the different elementary steps in the activation process of ethylene polymerization for substituted complexes [Zr{1-Me_2Si(3-η^5-$C_9H_5R)_2$}Cl_2] (R = Et **3**, Me **4**, *n*Pr **5** and *n*Bu **6**) by commercial methylaluminoxane (MAO) have been studied by UV–vis spectroscopy. Addition of MAO in large excess ([Al]/[Zr] = 2000) at −78 °C yields a previously unreported intermediate in the activation process of metallocenes; this intermediate has an absorption band centered at λ = 639 nm. We report here the influence of the type of catalyst, ring substitution, type of cocatalyst and addition of THF on the activation process of these metallocenes.

Keywords: Metallocene; Methylaluminoxane; Reaction mechanisms; UV–vis spectroscopy; Polymerization

1. Introduction

Based on production data for 2000, 85–95 million tonnes of polyolefins (essentially homopolymers and copolymers of ethylene and propylene) are produced globally each year. A large number of new catalysts for olefin polymerization, classified as metallocene catalysts, have been prepared during the last decade [1]. The majority of these catalysts consist of a zirconium complex with the general formula $LL'ZrCl_2$ and these systems are activated by methylaluminoxane (MAO). The ligands L and L′ are typically equivalent or different dienyl ligands that may be linked together by a bridge. One of the most important factors in zirconocene complexes as catalysts in olefin polymerization is that they require the action of a cocatalyst. The development of metallocene catalysis for olefin polymerization is closely tied to the discovery and use of the cocatalyst methylaluminoxane. The full cocatalytic functionality of MAO towards zirconocenes is still not fully understood [2].

The elementary mechanism of metallocene activation by MAO has attracted the attention of numerous research groups [1b,3]. The presence of chromophoric aromatic ligands directly attached to the transition metal in metallocenes allows investigation by UV–vis spectroscopy of metallocene/MAO systems under conditions much closer to those of the polymerization. Indeed, the formation of various types of metallocene species upon increasing amounts of MAO has been studied by this technique [4,5]. The activation proceeds in three successive steps, depending on the [MAO]/[Zr] ratio: (1) monoalkylation of the zirconocene dichloride, (2) formation of inactive electrodeficient zirconocene species and (3) formation of the catalytically active metallocenium species.

* Corresponding author. Tel.: +34 9 26295300; fax: +34 9 26295318.
E-mail address: Antonio.Otero@uclm.es (A. Otero).

1381-1169/$ – see front matter © 2006 Elsevier B.V. All rights reserved.
doi:10.1016/j.molcata.2006.07.041

With the above information in mind, we embarked in the first part of this work on the synthesis, characterization and catalytic activity of a new *ansa*-zirconocene [Zr{1-Me_2Si(3-η^5-$C_9H_5Et)_2$}Cl_2] (**3**) and in the second part in the study of the different elementary steps in the activation process of a series of *ansa*-zirconocenes [Zr{1-Me_2Si(3-η^5-$C_9H_5R)_2$}Cl_2] (R = Me, Et, *n*Pr and *n*Bu) [6] by MAO through the use of UV–vis spectroscopy. Finally, a comparison between [Zr{1-Me_2Si(3-η^5-$C_9H_5R)_2$}Cl_2]/MAO (R = Me, Et, *n*Pr and *n*Bu) and other related systems will also be made.

2. Experimental

2.1. General procedures

All reactions were carried out using standard Schlenk tube and glove box techniques in an atmosphere of dry nitrogen. Solvents were distilled from appropriate drying agents and degassed before use. $ZrCl_4$, indene, $SiMe_2Cl_2$, MeMgBr and $BrCH_2CH_3$ were purchased from Aldrich and used directly.

^{1}H and ^{13}C spectra were recorded on Varian UNITY FT-300 and Varian GEMINY FT-400 spectrometers and referenced to the residual deuterated solvent. Microanalyses were carried out with a Perkin-Elmer 2400 microanalyzer. Mass spectrometric analyses were performed on a Hewlett-Packard 5988A spectrometer (*m*/*z* 50–1000) (electron impact).

2.2. Preparation of compounds

2.2.1. Preparation of {1-Me_2Si(3-$C_9H_6Et)_2$} (**1**)

*n*BuLi (1.60 M in hexane) (38.00 ml, 60.74 mmol) was added over 15 min to a cooled (−78 °C) solution of [$Me_2Si(C_9H_7)$] (7.30 g, 25.31 mmol) in Et_2O (100 ml) in a 250 ml Schlenk tube. At the end of the addition, the solution was allowed to reach room temperature and stirred for 4 h, cooled again to −78 °C and $BrCH_2CH_3$ (11.13 g, 101.24 mmol) was added. The reaction mixture was allowed to reach room temperature and stirred for 16 h. The solvent was removed in vacuo and hexane (100 ml) was added. Water (200 ml) was added, the organic product was extracted with hexane and the aqueous layer was washed with hexane (3 × 50 ml). The combined organic layers were dried over $MgSO_4$, filtered and the solvent removed under reduced pressure to yield the title compound as yellow oil. Compound **1** was purified by column chromatography (Et_2O:hexane 1:9) (7.58 g, 87%).

^{1}H NMR (400 MHz, $CDCl_3$) (for the predominant isomer): δ 0.19 and 0.33 (2s, each 3H, $SiMe_2$), 0.90 (m, 6H, $-CH_2CH_3$), 1.34–2.74 (m, 4H, $-CH_2CH_3$), 3.59 (d, J = 1.8 Hz, 2H, H^1), 6.96 (d, J = 1.8 Hz, 2H, H^2), 7.10–7.50 (m, 8H, H^4–H^7). MS electron impact (*m*/*e* (relative intensity)): 344 (5) (M^+, {1-Me_2Si(3-$C_9H_6Et)_2$}$^+$), 202 (100) (M^+–(3-C_9H_6Et)), 144 (42) (M^+–Me_2Si).

2.2.2. Preparation of Li_2{1-Me_2Si(3-$C_9H_5Et)_2$} (**2**)

*n*BuLi (1.60 M in hexane) (21.05 ml, 33.67 mmol) was added dropwise over 15 min to a cooled (−78 °C), stirred solution of {1-Me_2Si(3-$C_9H_6Et)_2$} (**1**) (5.00 g, 15.80 mmol) in Et_2O (80 ml) in a 250 ml Schlenk tube. The solution was allowed to warm up to room temperature and stirred for 4 h. An increasing turbidity developed until a yellow-orange suspension had formed. The solvent was removed in vacuo to give a yellow solid, which was washed with hexane (2 × 50 ml) and dried under vacuum to yield **2** as a free flowing yellow solid (3.94 g, 76%). $C_{22}H_{22}Li_2Si$ (328.18): calcd. C 80.87, H 7.35; found C 80.73, H 7.29.

2.2.3. Preparation of [Zr{1-Me_2Si(3-η^5-$C_9H_5Et)_2$}Cl_2] (**3**)

A cooled (−78 °C) slurry of $ZrCl_4$ (2.58 g, 11.05 mmol) in toluene (80 ml) was added rapidly to a cooled (−78 °C) suspension of Li_2{1-Me_2Si(3-$C_9H_5Et)_2$} (**2**) (3.94 g, 11.05 mmol) in Et_2O (80 ml) in a 250 ml Schlenk tube. The reaction mixture was stirred for 30 min at −20 °C and then overnight at room temperature (16 h).

The orange suspension was filtered through a G4 frit with Celite. The filtrate was evaporated to dryness under reduced pressure to yield a sticky dark-orange product, which was washed with 30 ml of Et_2O. The residue was dried to give an orange solid (1.67 g, 30%). *rac*:*meso* = 71:29.

2.2.3.1. Meso isomer. ^{1}H NMR (400 MHz, $CDCl_3$): δ 0.91 (s, 3H, Si(CH_3) exo), 1.36 (s, 3H, Si(CH_3) endo), 1.21 (t, J = 7.9 Hz, 6H, CH_2CH_3), 2.80 (m, 4H, CH_2CH_3), 5.62 (s, 2H, H^2), 6.92 and 7.18 (2t, J = 8.8 Hz, each 2H, H^5, H^6), 7.45 and 7.48 (2d, J = 8.8 Hz, each 2H, H^4, H^4). ^{13}C NMR (100 MHz, $CDCl_3$): δ −2.54 (Si(CH_3) exo), −1.02 (Si(CH_3) endo), 14.08 (CH_2CH_3), 21.59 (CH_2CH_3), 116.05 (C^2), 124.02 and 125.80 (C^5, C^6), 126.25, 126.22 (C^4, C^7).

2.2.3.2. Racemic isomer. ^{1}H NMR (400 MHz, $CDCl_3$): δ 1.10 (s, 6H, Si(CH_3)$_2$), 1.11 (s, 6H, CH_2CH_3), 2.75 (m, 4H, $-CH_2CH_3$), 5.82 (s, 2H, H^2), 7.05 and 7.31 (2t, J = 8.8 Hz, each 2H, H^5, H^6), 7.45 and 7.48 (2d, J = 8.8 Hz, each 2H, H^4, H^7). ^{13}C NMR (100 MHz, $CDCl_3$): δ −1.36 (Si(CH_3)$_2$), 13.93 (CH_2CH_3), 21.31 (CH_2CH_3), 116.65 (C^2), 124.16 and 124.80 (C^5, C^6), 126.38 and 126.42 (C^4, C^7).

2.2.3.3. Both isomers. $C_{24}H_{26}Cl_2SiZr$ (504.68): calcd. C 57.12, H 5.19; found C 56.98, H 5.25.

2.2.4. Preparation of [Zr{1-Me_2Si(3-η^5-$C_9H_5nBu)_2$}$(CH_3)_2$] (**6b**)

MeMgBr (3 M in THF) (0.36 ml, 1.07 mmol) was added to a solution of **6** [Zr{1-Me_2Si(3-η^5-$C_9H_5nBu)_2$}Cl_2] [6] (0.30 g, 0.54 mmol) in THF (50 ml) at −78 °C. The reaction mixture was allowed to warm up to room temperature and stirred for 4 h. The solvent was removed in vacuo and hexane (25 ml) added. After filtration, the solution was concentrated to 5 ml and cooled at −20 °C overnight to afford the title complex (0.12 g, 42%).

2.2.4.1. Meso isomer. ^{1}H NMR (400 MHz, C_6D_6): δ −2.31 (s, 3H, Zr(CH_3) endo), −0.20 (s, 3H, Zr(CH_3) exo), 0.44 (s, 3H, Si(CH_3) exo), 0.80 (s, 3H, Si(CH_3) endo), 0.85 (t, J = 7.9 Hz, 6H, $CH_2CH_2CH_2CH_3$), 1.36 (m, 4H, $CH_2CH_2CH_2CH_3$), 1.55 (m, 4H, $CH_2CH_2CH_2CH_3$), 2.61 (m, 4H, $CH_2CH_2CH_2CH_3$),

5.31 (s, 2H, H_2), 6.82 and 6.99 (2t, $J = 7.8$ Hz, each 2H, H^5, H^6), 7.25 and 7.36 (2d, $J = 7.8$ Hz, each 2H, H^4, H^7). ^{13}C NMR (100 MHz, C_6D_6): δ −2.02 (Si(CH_3) exo), −1.42 (Si(CH_3) endo), 14.15 ($CH_2CH_2CH_2CH_3$), 23.10 ($CH_2CH_2CH_2CH_3$), 28.09 ($CH_2CH_2CH_2CH_3$), 33.27 ($CH_2CH_2CH_2CH_3$), 37.83 and 41.12 (Zr(CH_3)$_2$), 68.90 and 80.90 (C^1, C^3), 115.57 (C^2), 124.42 and 125.60 (C^5, C^6), 126.45, 126.33 (C^4, C^7).

2.2.4.2. Racemic isomer. ^{1}H NMR (400 MHz, C_6D_6): δ −1.16 (s, 6H, Zr(CH_3)$_2$), 0.60 (s, 6H, Si(CH_3)$_2$), 0.87 (s, 6H, $CH_2CH_2CH_2CH_3$), 1.36 (m, 4H, $CH_2CH_2CH_2CH_3$), 1.55 (m, 4H, $CH_2CH_2CH_2CH_3$), 2.91 (m, 4H, $CH_2CH_2CH_2CH_3$), 5.62 (s, 2H, H^2), 6.80 and 7.01 (2t, $J = 7.8$ Hz, each 2H, H^5, H^6), 7.20 and 7.40 (2d, $J = 7.8$ Hz, each 2H, H^4, H^7). ^{13}C NMR (100 MHz, C_6D_6): δ −1.61 (Si(CH_3)$_2$), 14.08 ($CH_2CH_2CH_2CH_3$), 22.97 ($CH_2CH_2CH_2CH_3$), 27.99 ($CH_2CH_2CH_2CH_3$), 33.13 ($CH_2CH_2CH_2CH_3$), 39.47 (Zr(CH_3)$_2$), 68.90 and 81.00 (C^1, C^3), 117.44 (C^2), 124.07 and 124.71 (C^5, C^6), 126.48 and 126.51 (C^4, C^7).

2.2.4.3. Both isomers. $C_{24}H_{26}Cl_2SiZr$ (504.68): calcd. C 69.30, H 7.75; found C 69.48, H 7.85.

2.3. Polymerization experiments

Polymerizations (three runs for catalyst) were carried out in a 250 ml glass reactor using toluene as solvent (100 ml). Catalysts (6 μmol) were treated with the appropriate quantity of a solution of MAO in toluene (10% Al, CROMPTON) for 15 min. Toluene (80 ml), TIBA (Al(iBu)$_3$) scavenger (2 ml) and activated catalyst were introduced, in this order, into the reactor and temperature was maintained at 343 K. The nitrogen atmosphere was removed and a continuous flow of ethylene (1.5 bar) was introduced during 30 min. The reaction mixture was then quenched by the addition of acidified methanol. The polymer was collected by filtration, washed with methanol and dried under vacuum at room temperature for 24 h.

2.4. UV–vis spectroscopy

For the UV–vis measurements, a metallocene–toluene solution (4.2×10^{-4} mol$_{Zr}$/l) was transferred to a 1 cm path length quartz cell equipped with Teflon stoppers. The samples were analyzed using a Shimazu UV-2501PC spectrophotometer. Alternatively, MAO [Al]/[Zr] = 70, 140 and 2000 for complexes **3**–**6**, was injected to the measurement cells and the reactions were followed by scanning the UV–vis spectrum. All measurements were performed under inert conditions using dried toluene and THF.

2.5. X-ray crystal structure determination for meso-(3)

Intensity data were collected with a NONIUS-MACH3 diffractometer equipped with a graphite monochromator and Mo Kα radiation source (λ = 0.71073 Å) using an $\omega/2\theta$-scan technique. The final unit cell parameters were determined from 25 well-centred reflections and refined by least-squares methods. Data were corrected for Lorentz and polarization effects and semi-empirical absorption correction (Psi-scans) was made [7].

Table 1
Selected bond lengths (Å) and angles (°) for *meso*-(**3**)

	meso-(**3**)
Bond lengths	
Zr(1)–Cent(1)	2.248(3)
Zr(1)–Cent(2)	2.248(1)
av Zr(1)–C(Cent(1))*	2.562(6)
av Zr(1)–C(Cent(2))*	2.552(6)
Zr(1)–Cl(1)	2.393(2)
Zr(1)–Cl(2)	2.422(2)
Bond angles	
Cent(1)–Zr–Cent(2)	128.74(3)
Si(1)–C(1)–Cent(1)	163.6(4)
Si(1)–C(11)–Cent(2)	163.5(3)
Cl(1)–Zr–Cent(1)	107.43(5)
Cl(1)–Zr–Cent(2)	106.77(5)
Cl(2)–Zr–Cent(1)	106.06(6)
Cl(2)–Zr–Cent(2)	106.22(6)

Cent(1) is the centroid of C(1)–C(5) and Cent(2) is the centroid of C(12)–C(15).
* Average bond length between Zr(1) and the carbon atoms of the C_5 ring of the cyclopentadienyl moiety.

The structure was solved using the direct methods [8], completed by subsequent difference Fourier syntheses, and refined by full matrix least-squares procedures on F^2 [9]. All non-hydrogen atoms were refined with anisotropic thermal parameters. The hydrogen atoms were placed using a "riding model" and included in the refinement at calculated positions. Weights were optimized in the final cycles. Crystallographic data are given in Table 1.

3. Results and discussion

3.1. Synthesis and characterization of ansa-zirconocenes: [Zr{1-Me$_2$Si(3-η^5-C$_9$H$_5$Et)$_2$}Cl$_2$] and [Zr{1-Me$_2$Si(3-η^5-C$_9$H$_5$nBu)$_2$}(CH$_3$)$_2$]

The preparation of the substituted *ansa*-indene precursor {1-Me$_2$Si(3-C$_9$H$_6$Et))$_2$} (**1**) was achieved by alkylation of the dilithium salt of the corresponding derivative, generated with *n*BuLi in Et$_2$O, with a large excess of EtBr (Scheme 1). The zirconocene [Zr{1-Me$_2$Si(3-η^5-C$_9$H$_5$Et)$_2$}Cl$_2$] (**3**) was prepared as a mixture of its stereoisomers (*rac:meso* = 71:29) using the precursor {1-Me$_2$Si(3-C$_9$H$_6$Et)$_2$} (**1**). As shown in Scheme 1, the deprotonation of **1** with *n*BuLi gave the dilithium salt **2**, and subsequent reaction of this salt with $ZrCl_4$ in toluene gave the corresponding complex **3**.

The ^{1}H NMR spectrum of compound **1** shows the *meso*-isomer to be the major isomer, with two singlets for the *ansa*-bridge methyl groups, a doublet for H^1, a doublet for H^2 and four multiplets corresponding to the protons of the C_6 ring of the indenyl moiety.

The ^{1}H NMR spectrum for the *meso* isomer of complex **3** shows two singlets for the *ansa*-bridge methyl groups, a singlet for the proton of the indenyl C_5 ring and four multiplets corre-

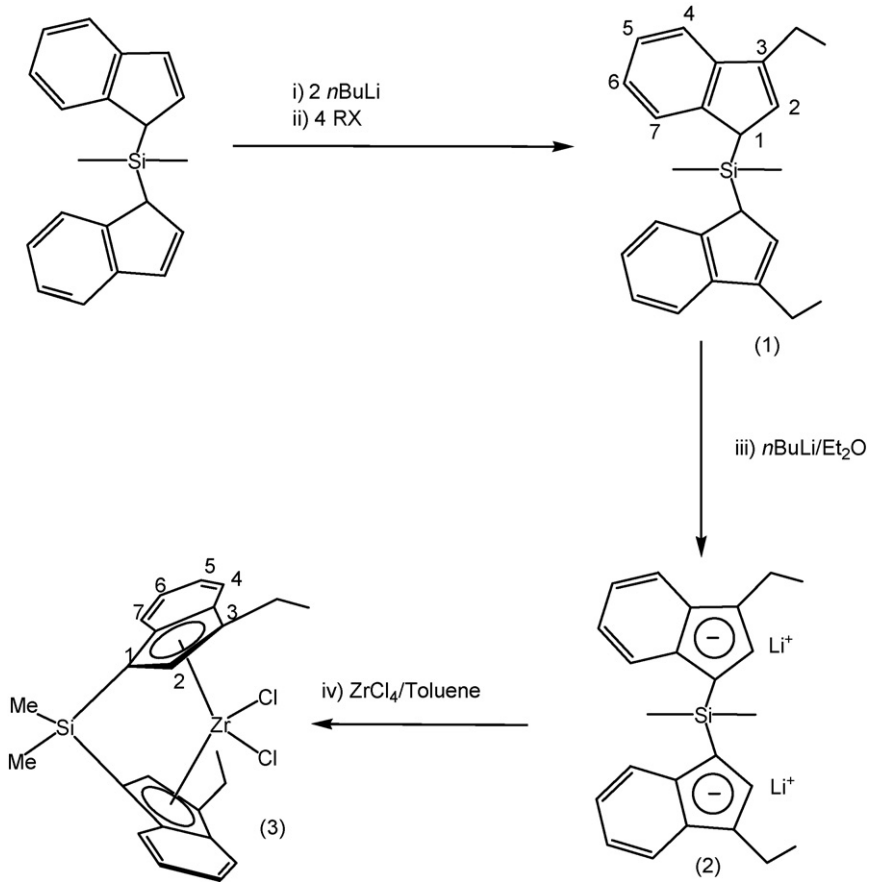

Scheme 1.

sponding to the protons of the C_6 ring of the indenyl moiety. In addition, signals were observed for the pendant alkyl chain. The *rac* isomer of complex **3** gave rise to a singlet for the *ansa*-bridge methyl groups, a singlet for the proton of the indenyl C_5 ring and four multiplets corresponding to the protons of the C_6 ring of the indenyl moiety. In addition, several signals were observed for the pendant alkyl chain.

^{1}H NMR nuclear overhauser effect (NOE) difference spectroscopy allowed unambiguous identification of each isomer. The carbon signal assignments were made using ^{1}H and ^{13}C NMR correlated spectroscopy (HETCOR) (see Section 2).

The preparation of the alkyl derivative [Zr{1-Me_2Si(3-η^5-C_9H_5nBu))$_2$}Me_2] (**6b**) was performed by the reacting the Grignard reagent MeMgBr with the corresponding dihalide *ansa*-zirconocene complex [Zr{1-Me_2Si(3-η^5-C_9H_5nBu)$_2$}Cl_2] [6] (Scheme 2). Compound **6b** was characterized by spectroscopic methods (see Section 2).

The ^{1}H NMR spectrum of **6b** was similar to that of the parent compound. In addition, a singlet for the metal-bonded equivalent methyl groups was observed for the *rac* isomer along with two singlets for the metal-bonded inequivalent methyl groups for the *meso* isomer.

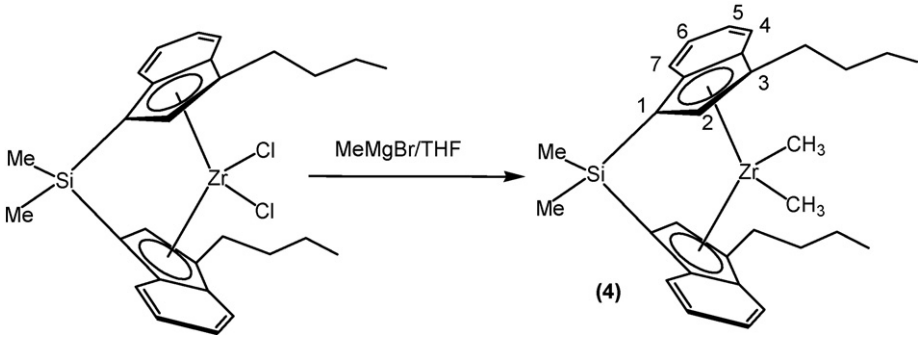

Scheme 2.

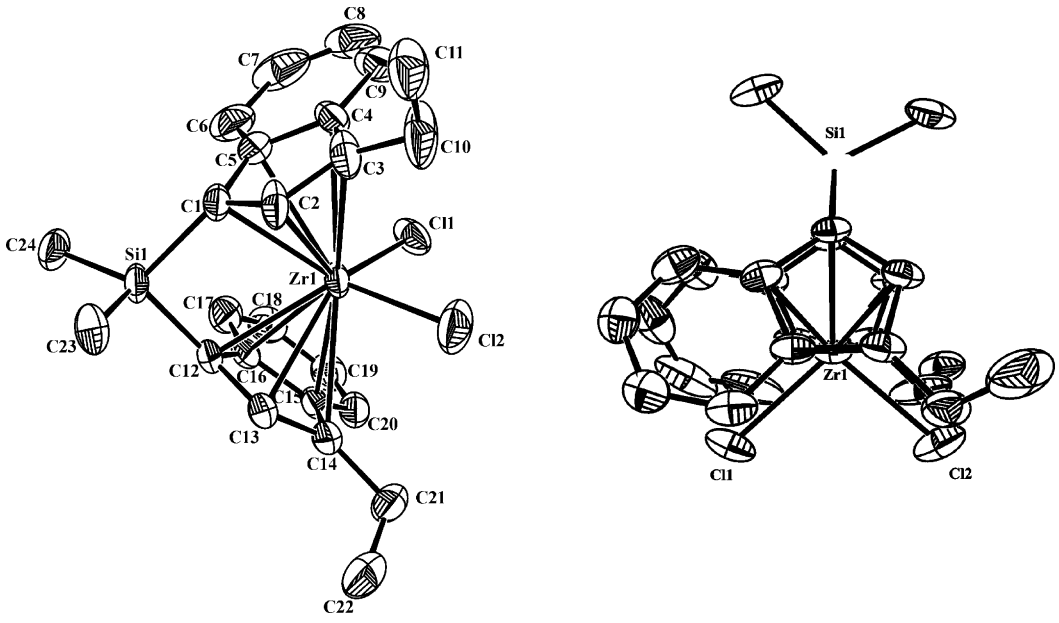

Fig. 1. Solid state structure of *meso*-(**3**) (hydrogen atoms are omitted for clarity).

Table 2
Homogeneous ethylene polymerization results for (**3**)

Complex	Activity ($kg_{PE}/mol_{Zr} \times h$)	Activity (after 12 h)* ($kg_{PE}/mol_{Zr} \times h$)
[Zr{1-$Me_2Si(3-\eta^5-C_9H_5Et)_2$}$Cl_2$] (**3**)	4173	2333
[Zr{1-$Me_2Si(\eta^5-C_9H_6)_2$}Cl_2]	3573	No reaction
[Zr{1-$C_2H_4(\eta^5-C_9H_6)_2$}Cl_2]	3500	No reaction

Data for [Zr{1-$Me_2Si(\eta^5-C_9H_6)_2$}Cl_2] and [Zr{1-$C_2H_4(\eta^5-C_9H_6)_2$}Cl_2] are included as references. Conditions: 343 K, 1.5 bar monomer pressure, 6 μmol Zr, MAO/Zr = 2000, 100 ml toluene and t_{pol} = 30 min.
* See the text.

3.2. X-ray molecular analysis of complex meso-(3)

Single crystals of *meso*-(**3**) that were suitable for X-ray diffraction were obtained from CH_2Cl_2/ether.

meso-(**3**) crystallizes in the triclinic space group $P\bar{1}$. This crystal structure reveals the existence of a single isomer. Two different ORTEP views are shown in Fig. 1. The zirconium atom is in a pseudotetrahedral environment formed by the two chlorine ligands and two η^5-coordinated indenyl ligands. The bonding parameters for *meso*-(**3**) are summarized in Table 2.

The Zr–C bond lengths of the five-membered rings range between 2.488 and 2.666 Å. This range is close to that in the *ansa*-bis(indenyl) zirconocene complexes (2.5 Å) [10]. The Zr–Cl distances are within the range observed previously for other bis(indenyl)-zirconium dichlorides [2.394(2)–2.422(2) Å] [11–16]. The mutual arrangement of the indenyl fragments corresponds to C_s symmetry. It can be seen from Fig. 1 that the two C_5 rings are eclipsed in the structure.

3.3. Catalytic properties of complex 3

Complex **3**, after activation with methylaluminoxane (MAO), is a very active catalyst for the polymerization of ethylene. In the present study, we used a commercial (CROPTOM) 10% solution of MAO in toluene, which contains about 20–30% of $AlMe_3$. In all polymerization experiments, $Al(^iBu)_3$ was used to scavenge possible impurities in the monomer and the solvent. The polymerization results are compared with those for two of the best known zirconocene catalysts, i.e., [Zr{1-$Me_2Si(\eta^5-C_9H_6)_2$}Cl_2] [17] and [Zr{1-$C_2H_4(\eta^5-C_9H_6)_2$}Cl_2] [18]. The polymerization results are shown in Table 3. Complex **3** is more active than the reference complexes [Zr{1-$Me_2Si(\eta^5-C_9H_6)_2$}Cl_2] and [Zr{1-$C_2H_4(\eta^5-C_9H_6)_2$}Cl_2].

The stability of metallocene complexes is one of the most important variables in terms of future industrial use. The activity of the activated form of complex **3** was tested after 12 h of contact with MAO solution. In this respect it is worth highlighting that complex **3** maintained a reasonable level of activity (56%) after this contact time. In marked contrast, the reference complexes [Zr{1-$Me_2Si(\eta^5-C_9H_6)_2$}Cl_2] and [Zr{1-$C_2H_4(\eta^5-C_9H_6)_2$}Cl_2] did not give any reaction with ethylene after prolonged contact with MAO.

Table 3
Activity ($kg_{PE}/mol_{Zr} \times h$) of **6** at different [Al]/[Zr] ratios

Complex	[Al]/[Zr] = 70	[Al]/[Zr] = 140	[Al]/[Zr] = 500	[Al]/[Zr] = 1000	[Al]/[Zr] = 2000
6	No reaction	No reaction	606	2000	2333

Conditions: 343 K, 1.5 bar monomer pressure, 6 μmol Zr, 100 ml toluene and t_{pol} = 30 min.

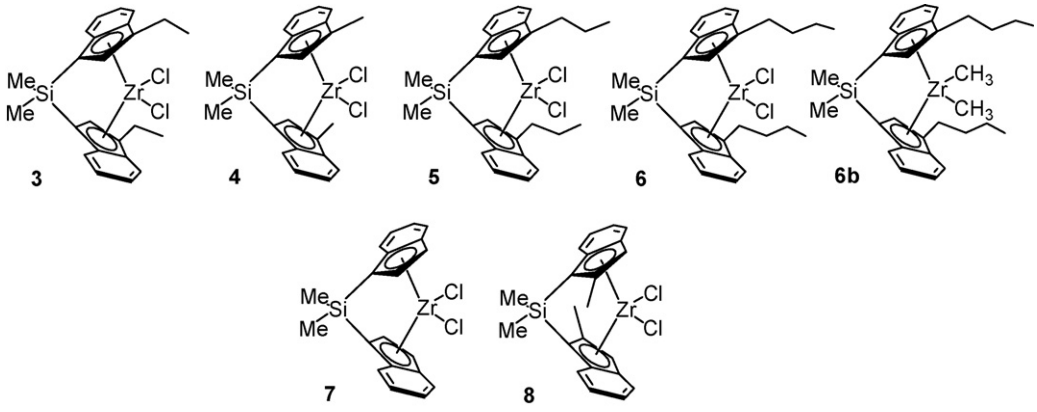

Scheme 3.

3.4. UV–vis spectroscopy studies

In a recent paper [6], we reported the synthesis, characterization and catalytic properties of a new family of 3-substituted *ansa*-bis-indenyl zirconocene complexes, [Zr{1-Me_2Si(3-η^5-$C_9H_5R)_2$}Cl_2] (R = Me, *n*Pr and *n*Bu). That study is completed here by the synthesis, structural characterization and assessment of the catalytic properties of the complex [Zr{1-Me_2Si(3-η^5-$C_9H_5Et)_2$}Cl_2].

The series of metallocene complexes shown in Scheme 3 was used in the UV–visible studies related to the activation process; namely *ansa*-zirconocenes substituted in position 3 with an alkyl chain (**3**–**6**), dimethyl derivative of **6** (**6b**), unsubstituted *ansa*-bis-indenyl zirconocene (**7**) and *ansa*-bis-indenyl zirconocene substituted in position 2 with a methyl group (**8**) [19].

The UV–vis spectra of complexes **3**–**6**, recorded in toluene at room temperature, are shown in Fig. 2.

For complexes **3**–**6**, the absorption spectra contain a main band located at 460 nm and there is no significant difference between the spectra of these compounds, as shown in Fig. 2. In addition, significant differences were not found between the absorption spectrum of a mixture enriched in the *meso*-**4** isomer and the same complex with an almost 1:1 *rac:meso* ratio (Fig. 3). Given this observation, the absorption spectra of complex **6** (as a mixture of isomers) are shown in this paper as representative examples for this family.

The absorption spectrum of **6** in toluene is characterized by a main band with a maximum located at 460 nm. The change in the position of the zirconocene absorption band after the addition of increasing amounts of MAO was investigated.

$$[Al]/[Zr] = 70$$

The influence of the addition of a small proportion of MAO ([Al]/[Zr] = 70) on the UV–vis absorption spectrum of the initial dichloride complex **6** can be seen in Fig. 4. Addition of the first portion of MAO leads to an extinction of the initial band in favour of a new band located at 420 nm (Fig. 4b).

It has been shown by ^{1}H NMR spectroscopy [20] that trimethylaluminum (TMA), which is present in commercial MAO, reacts with metallocene dichlorides and gives substitution of one chloro-substituent on the metal by a methyl group (monomethylation). In order to clarify this situation, we prepared the dimethylated complexes of **6**. Dimethylzirconocene **6b** was characterized (Fig. 5a) by an absorption band located at 390 nm, which is clearly distinct from the band observed for the derivative formed upon the addition of a small amount of MAO to **6** (420 nm) (Fig. 5b). On the basis of these results, we can assume that the metallocene species responsible for the absorption band at 420 nm is probably a monomethylated zirconocene species (see Fig. 5). It is worth noting that the formation of

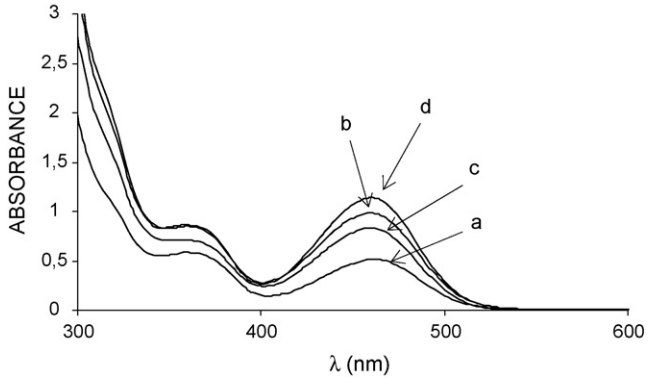

Fig. 2. UV–vis absorption spectrum of dichloride metallocenes: (a) **4** in toluene at room temperature, [**4**] = 4.2 × 10^{-5} M, (b) **3** in toluene at room temperature, [**3**] = 4.2 × 10^{-5} M, (c) **5** in toluene at room temperature, [**5**] = 4.2 × 10^{-5} M and (d) **6** in toluene at room temperature, [**6**] = 4.2 × 10^{-5} M.

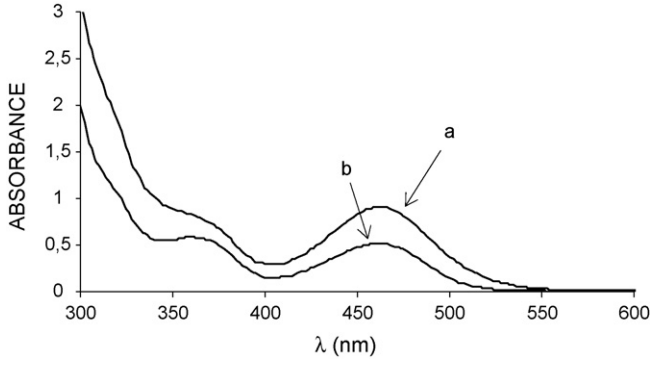

Fig. 3. UV–vis absorption spectrum of dichloride metallocenes: (a) **4** in a ratio *rac:meso* 2:98 and (b) **4** in a ratio *rac:meso* 55:45.

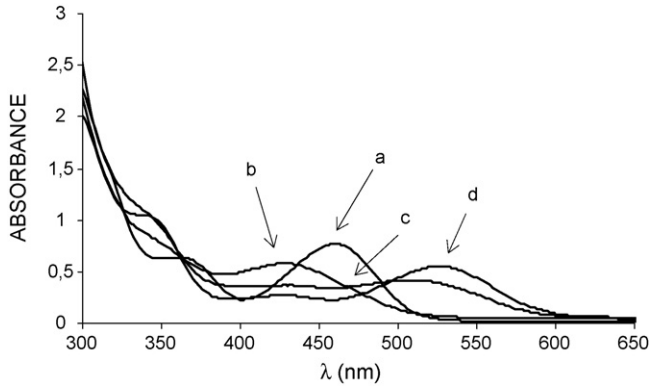

Fig. 4. UV–vis absorption spectrum of **6** in the presence of MAO in toluene at room temperature, [**6**] = 4.2×10^{-5} M: (a) [Al]/[Zr] = 0, (b) [Al]/[Zr] = 70, (c) [Al]/[Zr] = 140 and (d) [Al]/[Zr] = 2000.

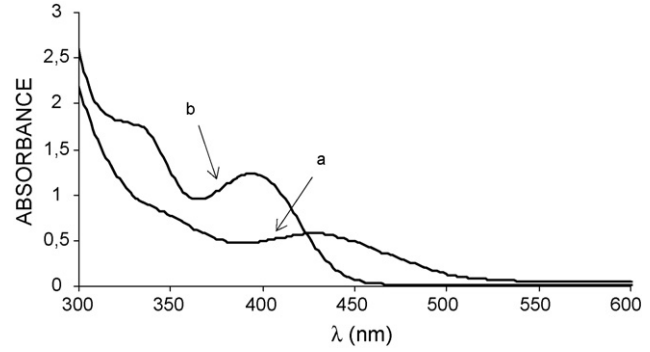

Fig. 5. (a) UV–vis absorption spectrum of **6** in the presence of MAO in toluene at room temperature: [**6**] = 4.2×10^{-5} M, [Al]/[Zr] = 70 and (b) UV–vis absorption spectrum of **6b**.

this proposed monomethylated complex is also observed after the addition of few equivalents of trimethylaluminum (TMA, [Al]/[Zr] = 100). The signal at 420 nm remains even after the addition of a large amount of crude TMA—a situation in agreement with the ineffectiveness of TMA to act as an ionizing agent for these zirconocenes.

[Al]/[Zr] = 140

The addition of larger amounts of MAO to the solution is accompanied by a reverse shift of the initial zirconocene absorption band. As shown in Fig. 4c, a bathochromic shift of the metallocene spectrum is observed. At [Al]/[Zr] = 140 it can be seen that the absorption band at 420 nm is progressively transformed into a new band characterized by a maximum located at 510 nm (Fig. 4c). We propose that this absorption band corresponds to a cationic contact species, as depicted in the scheme of Fig. 6.

[Al]/[Zr] = 2000

For higher [Al]/[Zr] ratios, the maximum located at 510 nm begins to continuously shift towards higher wavelengths until it finally reaches an upper limit located at 525 nm. It can be assumed that this absorption band would correspond to the final cationic species depicted in scheme of Fig. 6.

These intermediate species proposed in the activation mechanism are consistent with those proposed by Deffieux and co-workers [5] in the activation process of *rac*-[Zr{1-C_2H_4(η^5-C_9H_5)$_2$}Cl_2] by MAO: (1) generation of a neutral monomethyl monochloride zirconocene species at [Al]/[Zr] < 30, resulting in a band shift to higher energies (a hypsochromic shift), (2) with an increasing [Al]/[Zr] ratio of 30–150, a shift to lower energies was observed (bathochromic shift) and (3) at even higher ratios, [Al]/[Zr] = 150–2000, a second bathochromic shift of the band was observed. The bathochromic shift observed in the [Al]/[Zr] ratio range of 30–150 was concluded to be an indication of cation formation and the second bathochromic shift at [Al]/[Zr] = 150–2000 an indication of cation dissociation.

On the other hand, we also demonstrated that larger amounts of MAO are required to obtain the maximum activity plateau, the limit of which was located near [Al]/[Zr] = 2000 (Table 4).

It is worthy to emphasize the presence of an initial band in the UV–vis spectra of complexes **3**–**6** after reaction with MAO

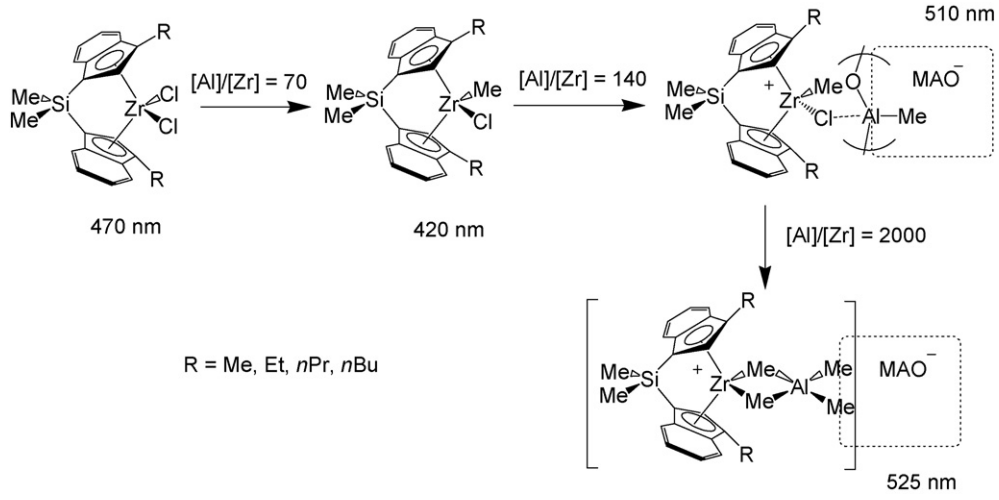

Fig. 6. Proposed mechanism for the activation process of **3**–**6** in the presence of MAO.

Table 4
Activity ($kg_{PE}/mol_{Zr} \times h$) of **6** at different cocatalysts and [Al]/[Zr] ratios

Cocatalyst	[Al]/[Zr] = 200	[Al]/[Zr] = 2000
Commercial MAO	367	2946
MAO(-TMA)	2360	2302

Conditions: 343 K, 1.5 bar monomer pressure, 6 μmol Zr, 100 ml toluene and t_{pol} = 30 min.

with a ratio of [Al]/[Zr] = 2000 at room temperature. This band disappeared after few seconds. However, it was possible to stabilize this band at −78 °C. The evolution of the UV–vis spectra of **6** is shown in Fig. 7 as a representative example. On reaction with MAO at −78 °C, the initial yellow toluene solution of the **6** dichloride species turned deep blue. Disappearance of the band at 460 nm and apparition of a new band at 639 nm was observed (Fig. 7b). We tentatively assign this band to a new intermediate of activation. At room temperature, the maximum located at 639 nm shifts towards lower wavelengths until it finally reaches a limit located at 525 nm; this absorption maximum at 525 nm correspond to the final proposed red cationic Zr(IV) active species (Fig. 7c). In any case, the formation of the monomethyl intermediate species was observed. Although we cannot rule out the possibility that a reduction process to Zr(III) takes place, even at this very low temperature, it seems very difficult to understand that, in a reducing medium as it is the MAO solution, the hypothetical reduced intermediate regenerates a Zr(IV) species. Furthermore, reaction with an excess of a well-established reductor as TMA, either low or room temperature, does not give rise to the observation of a band near 639 nm. In addition, hypsochromic shifts are proposed to be due [5] to an increase in the electronic density around the zirconium centre (as commented above for the spectra assigned to dimethyl and monomethyl species). Following this reasoning, a bathochromic shift to 639 nm is hardly assigned to any reduced, electron rich, Zr(III) compound.

The activation process by MAO on **6b**, which is characterized by an absorption band located at 390 nm (Fig. 5b), was investigated by UV–vis spectroscopy. The activation step is characterized by a bathochromic shift of the zirconocene main

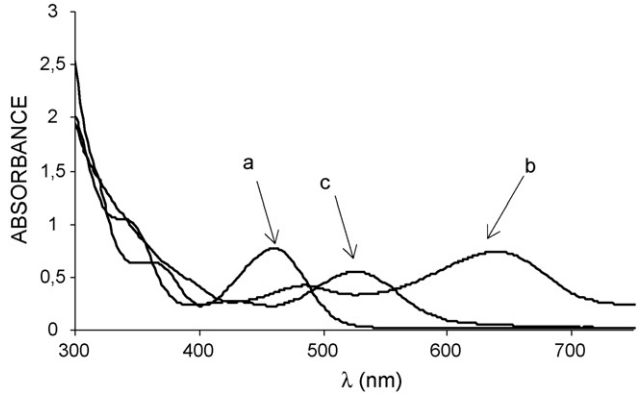

Fig. 7. UV–vis absorption spectrum of **6** in the presence of MAO in toluene, [**6**] = 4.2×10^{-5} M: (a) [Al]/[Zr] = 0 at room temperature, (b) [Al]/[Zr] = 2000 at −78 °C and (c) [Al]/[Zr] = 2000 after 2 min at room temperature.

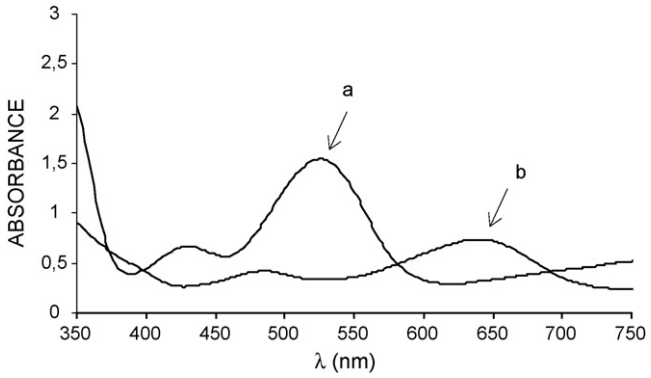

Fig. 8. (a) UV–vis absorption spectrum of **6b** in the presence of MAO in toluene at −78 °C, [**6b**] = 4.2×10^{-5} M, [Al]/[Zr] = 2000 and (b) UV–vis absorption spectrum of **6** in the presence of MAO in toluene at −78 °C, [**6**] = 4.2×10^{-5} M, [Al]/[Zr] = 2000.

absorption band from 390 to 525 nm, even at −78 °C (Fig. 8a). It is interesting to note that in this case neither the new blue intermediate nor the band at 510 nm has been observed.

In a similar way, when an excess of MAO was added at −78 °C to the monomethyl intermediate from **6**, identified by a band at 420 nm, the band at 525 nm corresponding to the final active species was observed immediately, but any band near 640 nm could be observed.

Pakkanen and co-workers have carried out extensive studies, by means of a combined UV–vis spectroscopic and theoretical methods, concerning the influence of substituents on the activation of zirconocene polymerization catalysts with MAO [21].

In our study, the experiments performed on **3**–**6** were also carried out with similar complexes that had different ring substituents. In the study of the activation process for the reference complex $[Zr\{1\text{-}Me_2Si(\eta^5\text{-}C_9H_6)_2\}Cl_2]$ (**7**) (non-substituted) (Fig. 9b), an absorption near 640 nm corresponding to a possible blue intermediate was not observed. The same result was found when the experiment was carried out on the 2-substituted complex $[Zr\{1\text{-}Me_2Si(2\text{-}Me\text{-}(\eta^5\text{-}C_9H_5))_2\}Cl_2$ (Fig. 9c). This specific observation allows us to suggest that the presence of the substituent in position 3 of the cyclopentadienyl ring is a crucial factor to observe this band a 640 nm.

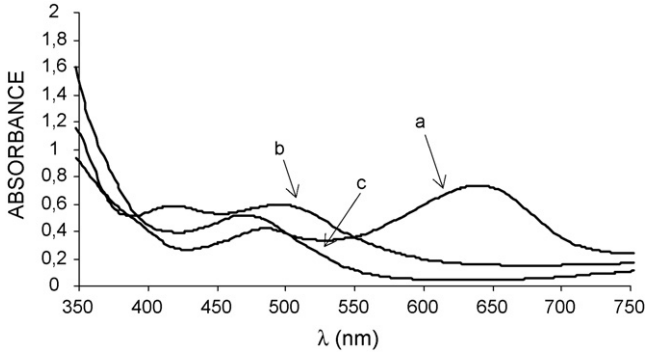

Fig. 9. (a) UV–vis absorption spectrum of **6** in the presence of MAO in toluene at −78 °C, [M4] = 4.2×10^{-5} M, [Al]/[Zr] = 2000, (b) UV–vis absorption spectrum of **7** in the presence of MAO in toluene at −78 °C, [**7**] = 4.2×10^{-5} M, [Al]/[Zr] = 2000 and (c) UV–vis absorption spectrum of **8** in the presence of MAO in toluene at −78 °C, [**8**] = 4.2×10^{-5} M, [Al]/[Zr] = 2000.

In order to study the possible influence of the cocatalyst on the observation of this new blue intermediate, we used MAO(-TMA) and TMA as cocatalysts to perform the same experiments. We prepared MAO(-TMA) from commercial MAO. Commercial MAO solutions contain a high percentage of TMA, which results from a partial hydrolysis process. TMA in MAO solutions can exist as two distinct forms: as free TMA (mainly in a dimeric form) and as complexed TMA (associated with MAO chains). The preparation of MAO(-TMA) by pumping off TMA from commercial solutions has been reported by several groups [22]. The solvent was removed at room temperature under reduced pressure to leave a residual off-white gel, which was maintained at 80 °C under reduced pressure for several hours to eliminate TMA. This process gave a white powder, which was stored in a glove box. The ^{1}H NMR spectrum of the recovered MAO shows that the amount of free TMA had been greatly reduced, but the removal of TMA was not complete. The use of MAO(-TMA) in the reaction with **6** at −78 °C gave rise to the appearance of the absorption band in the UV–vis spectrum corresponding to the new blue intermediate. Nevertheless, the existence of residual TMA in the MAO(-TMA) does not guarantee that the MAO rather than TMA is responsible for the formation of the blue intermediate. When an excess of TMA ([Al]/[Zr] = 2000) was used at −78 °C there was no apparent change in the band corresponding to dichloride species **6**. Moreover, at room temperature the maximum located at 460 nm begins to continuously shift towards lower wavelengths until it finally reaches an upper limit located at 420 nm, which corresponds to the monomethyl derivative. On the basis of these results, we propose that the presence of MAO molecules is required for the formation of the blue intermediate, meanwhile that TMA is not enough acidic to be involved in the process.

The development of metallocenes as olefin polymerization catalysts on an industrial scale requires a marked decrease in the content of costly aluminum-based cocatalysts such as MAO. It is particularly necessary to explore new routes that allow the [Al]/[Zr] ratio to be minimized while maintaining optimal catalytic activity for olefin polymerization [22]. In this way, we also observed in the study that the dichloride species was active for low [Al]/[Zr] ratios when MAO(-TMA) [23] was used (see Table 5). These results are consistent with similar studies carried out by Deffieux and co-workers [23,24]. Although the exact structure of MAO has still not been completely elucidated, it has been shown that the structure can be greatly influenced by the amount of TMA present. Removal of TMA will lead to condensation of MAO chains, thus increasing the molar mass of the system. This condensation process is also likely to be accompanied by changes in the global MAO structure. The addition of MAO(-TMA) at [Al]/[Zr] ratios of about 200 to complexes **3**–**6** yields to new species that absorb in their spectra at around 485 nm. This latter species is highly active towards olefin polymerization. These differences indicate that the MAO structure plays an important role in the zirconocene activation process.

Barron and co-workers [25] observed that the addition of Al(^{t}Bu)$_3$ to [Zr(η^5-C$_5$H$_5$)$_2$X$_2$] (X = Me, Cl) yields the air-sensitive Lewis acid–base complex [(η^5-C$_5$H$_5$)$_2$ZrX(μ-X)-Al(^{t}Bu)$_3$] (X = Me, Cl). The molecular structure of [(η^5-C$_5$H$_5$)$_2$ZrCl(μ-Cl)-Al(^{t}Bu)$_3$] indicates the presence of a Zr(μ-Cl)Al moiety. In the case that the observed species, identified by a band at 640 nm, it could be a kind of adduct with some acidic aluminum centers in MAO, of such form that addition of an external base as THF could break this interaction. The intermediate solution changed color from blue to yellow when THF was added. A hypsochromic shift of the main zirconocene absorption band from 639 to 460 nm was observed (Fig. 10). The band at 460 nm, corresponding to the dichloride species, was maintained even when the temperature was reached, and the band at 525 nm, assigned to the active species was not observed. On this occasion, THF acts to poison the catalyst, i.e., occupying the most acidic centres in MAO. This observation provides further evidence for our hypothesis that the new blue intermediate is a type of labile adduct between these MAO acidic centers and

Table 5
Crystal data and structure refinement for *meso*-(**3**)

Empirical formula	$C_{24}H_{26}Cl_2SiZr$
Formula weight	504.66
Temperature (K)	290(2)
Wavelength (Å)	0.71073
Crystal system	Triclinic
Space group	$P\bar{1}$
a (Å)	12.925(4)
b (Å)	13.069(3)
c (Å)	14.819(3)
α (°)	106.83(1)
β (°)	103.69(2)
γ (°)	99.11(2)
Volume (Å^3)	2258(1)
Z	4
Density (calculated) (g/cm^3)	1.485
Absorption coefficient (cm^{-1})	7.85
F(0 0 0)	1032
Crystal size (mm^3)	0.3 × 0.2 × 0.2
Index ranges	$-17 \le h \le 16$; $-17 \le k \le 16$; $0 \le l \le 19$
Independent reflections	10812 [R(int) = 0.0351]
Data/restraints/parameters	10812/0/505
Goodness-of-fit on F^2	0.995
Final R indices [$I > 2\sigma(I)$]	R_1 = 0.0624, wR_2 = 0.1349
Largest diff. peak and hole (e.Å^{-3})	0.755 and −0.685

$R_1 = \Sigma||Fo|-|Fc||/\Sigma|Fo|$; $wR_2 = [\Sigma[w(Fo^2 - Fc^2)^2]/\Sigma[w(Fo^2)^2]^{0.5}$.

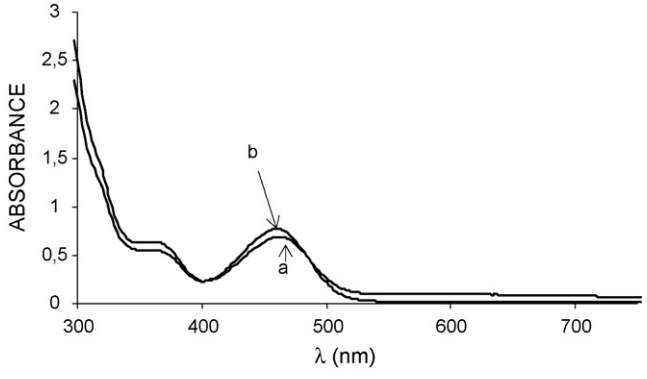

Fig. 10. (a) UV–vis absorption spectrum of **6** in toluene, [**6**] = 4.2 × 10^{-5} M and (b) UV–vis absorption spectrum of **6** in the presence of MAO in toluene at −78 °C after addition of THF, [**6**] = 4.2 × 10^{-5} M, [Al]/[Zr] = 2000.

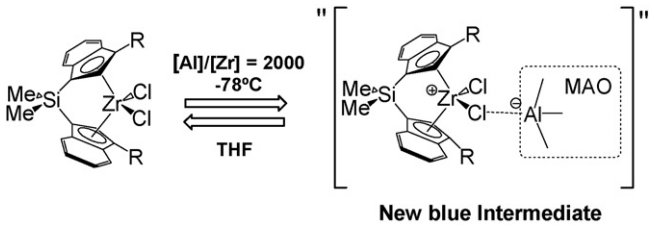

Scheme 4.

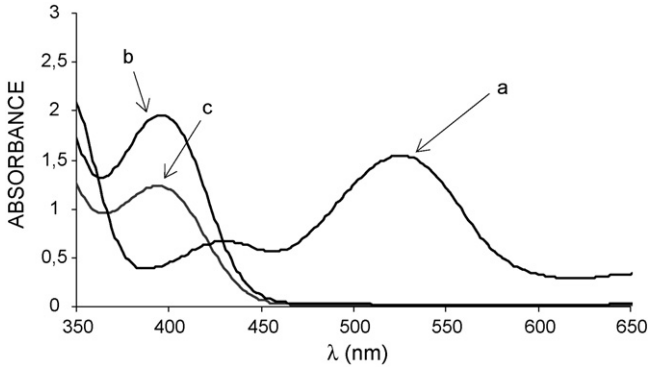

Fig. 11. (a) UV–vis absorption spectrum of **6** in the presence of MAO in toluene at room temperature, [**6**] = 4.2×10^{-5} M, [Al]/[Zr] = 2000, (b) 'a' after addition of THF, [**6**] = 4.2×10^{-5} M and (c) UV–vis absorption spectrum of **6b** in toluene at room temperature, [**6b**] = 4.2×10^{-5} M.

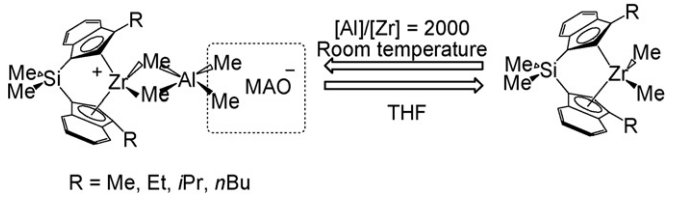

Scheme 5.

the dichloride metallocene complex. The new blue intermediate is reversibly converted to the dichloride species when THF is added (Scheme 4).

When THF was added to the active form of **6**, we observed a hypsochromic shift in the main zirconocene absorption band from 525 to 390 nm (Fig. 11), and the corresponding red toluene solution turned yellow. The band at 390 nm corresponds to the dimethyl species **6b** (note that the color of the toluene solution of **6b** was yellow). Barron and co-workers [25] observed the formation of [Zr(η^5-C_5H_5)$_2$Me$_2$] and Al(^{t}Bu)$_3$(L) (L = THF, MeCN) when external Lewis bases (THF, MeCN) were added to the Lewis acid–base complex [(η^5-C_5H_5)$_2$ZrMe(μ-Me)-Al(^{t}Bu)$_3$]. This result could also support the formation in our experiment of the dimethyl species (**6b**) when THF is added to the active species of **6b** (Scheme 5).

4. Conclusions

We have carried out the synthesis of new examples of *ansa*-bis-indenylzirconocenes complexes, bearing a $SiMe_2$ bridge, with alkyl substituents in the 3-position. In addition, complex *meso*-[Zr{1-Me_2Si(3-η^5-$C_9H_5(CH_2CH_3)$)$_2$}Cl_2] has been characterized by X-ray diffraction methods. This complex **3** is a very active catalyst, after MAO addition, in the catalytic polymerization of ethylene, even when long times of aging were used.

Finally, this study is delivering new spectroscopy data on the elementary steps leading to the formation to active species concerning *ansa*-bis-indenylzirconocenes/MAO systems. The presence of alkyl substituents in the 3-position of the cyclopentadienyl ring gives rise to the observation of a blue intermediate, before the observation of the active species.

Acknowledgements

We gratefully acknowledge financial support from the Ministerio de Educación y Ciencia, Spain (Grant No. MAT2003-05345), and the Junta de Comunidades de Castilla-La Mancha (Grant No. PBI05-029). C.A. and P.C. acknowledge a fellowship from REPSOL-YPF-UCLM (contracts CTR-00-084 and CTR-01-165).

References

[1] See reviews by:
(a) P.C. Möring, N.J. Coville, J. Organomet. Chem. 479 (1994) 1;
(b) H.-H. Brintzinger, D. Fischer, R. Mülhaupt, B. Rieger, R.M. Waymouth, Angew. Chem. 107 (1995) 1255;
H.-H. Brintzinger, D. Fischer, R. Mülhaupt, B. Rieger, R.M. Waymouth, Angew. Chem., Int. Ed. Engl. 34 (1995) 1143;
(c) T.J. Marks, J.C. Stevens (Eds.), Top. Catal. 7 (1999) 1.;
(d) J.A. Gladysz (Ed.), Chem. Rev. 100 (2000) 1167;
(e) M. Bochmann, J. Organomet. Chem. 689 (2004) 3982;
(f) W. Kaminsky, J. Polym. Sci. Part A: Polym. Chem. 42 (2004) 3911.
[2] E.Y.-X. Chen, Chem. Rev. 100 (2000) 1391.
[3] (a) H. Sinn, W. Kaminsky, H.J. Vollmer, R. Woldt, Angew. Chem. 92 (1980) 296;
(b) H. Sinn, W. Kaminsky, Adv. Organomet. Chem. 18 (1990) 99.
[4] P.J.J. Pieters, J.A.M. Van Beedk, M.F.H. Van Tol, Makromol. Chem., Rapid Commun. 16 (1995) 463.
[5] (a) D. Coevet, H. Cramail, A. Deffieux, Macromol. Chem. Phys. 199 (1998) 1459;
(b) J.-N. Pédeutour, D. Coevet, H. Cramail, A. Deffieux, Macromol. Chem. Phys. 1999 (200) 1215;
(c) J.-N. Pédeutour, K. Radhakrishnan, H. Cramail, A. Deffieux, Polym. Int. 51 (2002) 973.
[6] The synthesis and characterization of complexes 4, 5 and 6 have been described in: C. Alonso-Moreno, A. Antiñolo, F. Carrillo-Hermosilla, A. Otero, A.M. Rodríguez, J. Sancho, V. Volkis, M. Eisen, Eur. J. Inorg. Chem. (2006) 972.
[7] A.C.T. North, D.C. Phillips, F.S. Mathews, Acta. Crystallogr. A24 (1968) 351.
[8] SIR92, A program for crystal structure solution A. Altomare, G. Cascarano, C. Giacovazzo, A. Guagliardi, J. Appl. Crystallogr. 26 (1993) 343.
[9] G.M. Sheldrick, Program for the Refinement of Crystal Structures from Diffraction Data, University of Göttingen, Göttingen, Germany, 1997.
[10] (a) M. Toto, L. Cavallo, P. Corradini, G. Moscardi, L. Resconi, G. Guerra, Macromolecules 31 (1998) 3431;
(b) L. Resconi, D. Balboni, G. Baruzzi, C. Fiori, S. Guidotti, P. Mercandelli, A. Sironi, Organometallics 19 (2000) 420.
[11] (a) G. Erker, B. Temme, J. Am. Chem. Soc. 114 (1992) 4004;
(b) G. Erker, M. Aulbach, M. Knickmeier, D. Wingbermühle, C. Kruger, M. Nolte, S. Werner, J. Am. Chem. Soc. 115 (1993) 4590.
[12] C. Krüger, F. Lutz, M. Notle, G. Erker, M. Aulbach, J. Organomet. Chem. 452 (1993) 79.

[13] N.E. Grimmer, N.J. Coville, C.B. de Koning, J.M. Smith, L.M. Cook, J. Organomet. Chem. 616 (1993) 112.
[14] G. Jany, M. Gustafsson, T. Repo, E. Aitola, J.A. Dobado, M. Klinga, M. Leskelä, J. Organomet. Chem. 558 (1998) 11.
[15] R.L. Halterman, D.R. Fahey, E.F. Baillo, D.W. Docker, O. Stenzel, J.L. Shipman, M.A. Khan, S. Dechert, H. Suman, Organometallics 19 (2000) 5464.
[16] S. Knüppel, J.-L. Fauré, G. Erker, G. Kher, M. Nissinen, R. Fröhlich, Organometallics 19 (2000) 1262.
[17] W.A. Hermann, J. Rohrmann, E. Herdtweck, W. Spaleck, A. Winter, Angew. Chem., Int. Ed. Engl. 28 (1989) 1511.
[18] W. Kaminsky, K. Külper, H.-H. Brintzinger, F. Wild, Angew. Chem., Int. Ed. Engl. 24 (1985) 507.
[19] W. Spaleck, M. Antber, M. Rohrmann, A. Winter, B. Bachmann, P. Kiprof, J. Behm, W. Herrmann, Angew. Chem., Int. Ed. Engl. 31 (1992) 1347.
[20] (a) L. Resconi, S. Bossi, L. Abis, Macromolecules 223 (1990) 4489;
(b) D. Cam, U. Giannini, Makromol. Chem. 193 (1992) 1049.
[21] (a) N.I. Mäkela, H.R. Knuutila, M. Linnolahti, T.A. Pakkanen, J. Chem. Soc., Dalton Trans. (2001) 91;
(b) N.I. Mäkela, H.R. Knuutila, M. Linnolahti, T.A. Pakkanen, Macromolecules 35 (2002) 3395.
[22] (a) M.L. Ferreira, P.G. Belelli, D.E. Damiani, Macromol. Chem. Phys. 202 (2001) 495;
(b) Q. Wang, L. Song, Y. Zhao, L. Feng, Macromol. Rapid. Commun. 22 (2001) 1030;
(c) H. Cramail, A. Deffieux, J.-N. Pédeutour, K. Radhakrishnan, Macromol. Symp. 183 (2002) 113;
(d) H. Cramail, K. Radhakrishnan, A. Deffieux, C.R. Chimie 5 (2002) 49;
(e) K. Radhakrishnan, H. Cramail, A. Deffieux, P. Francois, A. Momtaz, Macromol. Rapid Commun. 23 (2002) 829.
[23] J.-N. Pédeutour, K. Radhakrishnam, H. Cramail, A. Deffieux, J. Mol. Catal. A: Chem. 185 (2002) 119.
[24] (a) J.-N. Pédeutour, H. Cramail, A. Deffieux, J. Mol. Catal. A: Chem. 174 (2001) 81;
(b) J.-N. Pédeutour, H. Cramail, A. Deffieux, J. Mol. Catal. A: Chem. 176 (2001) 87.
[25] C.J. Harian, S.G. Bott, A.R. Barron, J. Am. Chem. Soc. 117 (1995) 6465.